

TECHNICAL REPORT

Rare earth sintered magnets – Stability of the magnetic properties at elevated temperatures



THIS PUBLICATION IS COPYRIGHT PROTECTED

Copyright © 2009 IEC, Geneva, Switzerland

All rights reserved. Unless otherwise specified, no part of this publication may be reproduced or utilized in any form or by any means, electronic or mechanical, including photocopying and microfilm, without permission in writing from either IEC or IEC's member National Committee in the country of the requester.

If you have any questions about IEC copyright or have an enquiry about obtaining additional rights to this publication, please contact the address below or your local IEC member National Committee for further information.

Droits de reproduction réservés. Sauf indication contraire, aucune partie de cette publication ne peut être reproduite ni utilisée sous quelque forme que ce soit et par aucun procédé, électronique ou mécanique, y compris la photocopie et les microfilms, sans l'accord écrit de la CEI ou du Comité national de la CEI du pays du demandeur.

Si vous avez des questions sur le copyright de la CEI ou si vous désirez obtenir des droits supplémentaires sur cette publication, utilisez les coordonnées ci-après ou contactez le Comité national de la CEI de votre pays de résidence.

IEC Central Office
3, rue de Varembe
CH-1211 Geneva 20
Switzerland
Email: inmail@iec.ch
Web: www.iec.ch

About IEC publications

The technical content of IEC publications is kept under constant review by the IEC. Please make sure that you have the latest edition, a corrigenda or an amendment might have been published.

- Catalogue of IEC publications: www.iec.ch/searchpub

The IEC on-line Catalogue enables you to search by a variety of criteria (reference number, text, technical committee,...). It also gives information on projects, withdrawn and replaced publications.

- IEC Just Published: www.iec.ch/online_news/justpub

Stay up to date on all new IEC publications. Just Published details twice a month all new publications released. Available on-line and also by email.

- Electropedia: www.electropedia.org

The world's leading online dictionary of electronic and electrical terms containing more than 20 000 terms and definitions in English and French, with equivalent terms in additional languages. Also known as the International Electrotechnical Vocabulary online.

- Customer Service Centre: www.iec.ch/webstore/custserv

If you wish to give us your feedback on this publication or need further assistance, please visit the Customer Service Centre FAQ or contact us:

Email: csc@iec.ch
Tel.: +41 22 919 02 11
Fax: +41 22 919 03 00

TECHNICAL REPORT

Rare earth sintered magnets – Stability of the magnetic properties at elevated temperatures

INTERNATIONAL
ELECTROTECHNICAL
COMMISSION

PRICE CODE

U

ICS 29.030

ISBN 2-8318-1034-1

CONTENTS

FOREWORD.....	4
INTRODUCTION.....	6
1 Scope.....	7
2 Normative references	7
3 Terms and definitions	7
4 Classification of magnetic flux loss due to temperature.....	9
4.1 Reversible flux loss	9
4.2 Irreversible flux loss	9
4.3 Permanent flux loss.....	9
5 Long term ageing of rare earth magnets	10
6 Experimental	11
7 Temperature stability.....	13
7.1 Flux change due to temperature	13
7.2 Effect of temperature on B_r and H_{CJ} (demagnetization curves at different temperatures).....	14
7.3 The time effects at constant temperature (influence of temperature exposure and L/D)	16
7.4 The influence of H_{CJ} on the irreversible flux loss for Sm_2Co_{17} magnets	18
7.5 The influence of H_{CJ} on the irreversible flux loss for Nd-Fe-B magnets	20
7.6 Irreversible flux loss per decade	22
7.7 Permanent flux loss.....	22
8 Summary.....	24
Annex A (informative) Summary of temperature stability graphs.....	25
Annex B (informative) Non-linearity of temperature dependence of B_r and H_{CJ}	26
Bibliography.....	27
Figure 1 – Change of magnetic flux density operating on a load line during elevated temperature ageing after R. Tenzer (schematic) [7, 8]	10
Figure 2 – Long term ageing of rare earth magnets (schematic) [9].....	11
Figure 3 – Measuring system of open circuit flux utilizing a fluxgate type digital integrating fluxmeter [13]	12
Figure 4 – Temperature dependence of flux for $SmCo_5$ magnet ($L/D = 0,7$) [16] (See Table 1)	14
Figure 5 – Temperature dependence of flux for Sm_2Co_{17} magnet ($L/D = 0,7$) [16] (See Table 1)	14
Figure 6 – Temperature dependence of flux for Nd-Fe-B magnet ($L/D = 0,7$) [17] (See Table 1)	14
Figure 7 – J - H demagnetization curves of Nd-Fe-B magnet measured at different temperatures [18]	14
Figure 8 – J - H demagnetization curves of Nd-Fe-B magnet measured at different temperatures [19]	15
Figure 9 – Temperature dependence of normalized B_r and H_{CJ} for $SmCo_5$, Sm_2Co_{17} and Nd-Fe-B magnets [19].....	15
Figure 10 – Time dependence of irreversible flux loss for $SmCo_5$ magnet exposed at different temperatures [22].....	16
Figure 11 – Time dependence of irreversible flux loss for $SmCo_5$ magnets with various L/D s [24].....	16

Figure 12 – Time dependence of irreversible flux loss for $\text{Sm}_2\text{Co}_{17}$ magnet exposed at different temperatures (Material 1) [22]	17
Figure 13 – Time dependence of irreversible flux loss for $\text{Sm}_2\text{Co}_{17}$ magnets with various L/D s (Material 2) [24]	17
Figure 14 – Time dependence of irreversible flux loss for Nd-Fe-B magnet exposed at different temperatures [23]	17
Figure 15 – Temperature dependence of irreversible flux loss after exposure for 100 h for Nd-Fe-B magnets with various L/D s [25]	17
Figure 16 – Time dependence of irreversible flux loss for a $\text{Sm}_2\text{Co}_{17}$ magnet with $H_{\text{CJ}} = 0,48$ MA/m and $L/D = 0,7$ [26]	19
Figure 17 – Time dependence of irreversible flux loss for a $\text{Sm}_2\text{Co}_{17}$ magnet with $H_{\text{CJ}} = 1,19$ MA/m and $L/D = 0,7$ [27]	19
Figure 18 – Time dependence of irreversible flux loss for a $\text{Sm}_2\text{Co}_{17}$ magnet with $H_{\text{CJ}} = 1,97$ MA/m and $L/D = 0,7$ [28]	19
Figure 19 – Time dependence of irreversible flux loss for a Nd-Fe-B magnet with $H_{\text{CJ}} = 1,16$ MA/m and $L/D = 0,7$ [30]	20
Figure 20 – Time dependence of irreversible flux loss for a Nd-Fe-B magnet with $H_{\text{CJ}} = 1,66$ MA/m and $L/D = 0,7$ [31]	20
Figure 21 – Time dependence of irreversible flux loss for a Nd-Fe-B magnet with $H_{\text{CJ}} = 2,17$ MA/m and $L/D = 0,7$ [32]	21
Figure 22 – Time dependence of irreversible flux loss for a Nd-Fe-B magnet with $H_{\text{CJ}} = 2,45$ MA/m and $L/D = 0,7$ [33]	21
Figure 23 – Comparison of irreversible flux loss for $\text{Sm}_2\text{Co}_{17}$ magnets with different H_{CJ}	21
Figure 24 – Comparison of irreversible flux loss for Nd-Fe-B magnets with different H_{CJ}	21
Figure 25 – Relationship between irreversible flux loss per decade and initial flux loss	23
Figure B.1 – Temperature dependence of normalized B_r and H_{CJ} to show the non-linearity (see data for Nd-Fe-B magnets in Figure 9)	26
Table 1 – Magnetic properties of the rare earth magnets employed for the open circuit flux measurements to determine the reversible temperature coefficient of the magnetic flux	13
Table 2 – Reversible temperature coefficient of the magnetic flux determined by temperature cycling	13
Table 3 – Temperature coefficients of B_r and H_{CJ} for SmCo_5 , $\text{Sm}_2\text{Co}_{17}$ and Nd-Fe-B magnets (temperature range for the coefficient: 25 °C to 150 °C)	16
Table 4 – Magnetic properties of the specimens for the experiments to evaluate the effects of temperature and L/D on irreversible flux loss	18
Table 5 – Magnetic properties of the $\text{Sm}_2\text{Co}_{17}$ magnets for the experiment to evaluate the influence of H_{CJ} on the irreversible flux loss	20
Table 6 – The magnetic properties of Nd-Fe-B magnets for the evaluation of the influence of H_{CJ} on irreversible flux loss measured by a pulse recording fluxmeter	22
Table 7 – The permanent flux loss of $\text{Sm}_2\text{Co}_{17}$ magnets after exposure for 1 000 h at different temperatures	23
Table 8 – The permanent flux loss of Nd-Fe-B magnets after exposure for 1 000 h at different temperatures	23
Table 9 – Basic magnetic properties of the three intermetallic compounds	24
Table A.1 – Summary of temperature stability graphs	25

INTERNATIONAL ELECTROTECHNICAL COMMISSION

RARE EARTH SINTERED MAGNETS – STABILITY OF THE MAGNETIC PROPERTIES AT ELEVATED TEMPERATURES

FOREWORD

- 1) The International Electrotechnical Commission (IEC) is a worldwide organization for standardization comprising all national electrotechnical committees (IEC National Committees). The object of IEC is to promote international co-operation on all questions concerning standardization in the electrical and electronic fields. To this end and in addition to other activities, IEC publishes International Standards, Technical Specifications, Technical Reports, Publicly Available Specifications (PAS) and Guides (hereafter referred to as "IEC Publication(s)"). Their preparation is entrusted to technical committees; any IEC National Committee interested in the subject dealt with may participate in this preparatory work. International, governmental and non-governmental organizations liaising with the IEC also participate in this preparation. IEC collaborates closely with the International Organization for Standardization (ISO) in accordance with conditions determined by agreement between the two organizations.
- 2) The formal decisions or agreements of IEC on technical matters express, as nearly as possible, an international consensus of opinion on the relevant subjects since each technical committee has representation from all interested IEC National Committees.
- 3) IEC Publications have the form of recommendations for international use and are accepted by IEC National Committees in that sense. While all reasonable efforts are made to ensure that the technical content of IEC Publications is accurate, IEC cannot be held responsible for the way in which they are used or for any misinterpretation by any end user.
- 4) In order to promote international uniformity, IEC National Committees undertake to apply IEC Publications transparently to the maximum extent possible in their national and regional publications. Any divergence between any IEC Publication and the corresponding national or regional publication shall be clearly indicated in the latter.
- 5) IEC provides no marking procedure to indicate its approval and cannot be rendered responsible for any equipment declared to be in conformity with an IEC Publication.
- 6) All users should ensure that they have the latest edition of this publication.
- 7) No liability shall attach to IEC or its directors, employees, servants or agents including individual experts and members of its technical committees and IEC National Committees for any personal injury, property damage or other damage of any nature whatsoever, whether direct or indirect, or for costs (including legal fees) and expenses arising out of the publication, use of, or reliance upon, this IEC Publication or any other IEC Publications.
- 8) Attention is drawn to the Normative references cited in this publication. Use of the referenced publications is indispensable for the correct application of this publication.
- 9) Attention is drawn to the possibility that some of the elements of this IEC Publication may be the subject of patent rights. IEC shall not be held responsible for identifying any or all such patent rights.

The main task of IEC technical committees is to prepare International Standards. However, a technical committee may propose the publication of a technical report when it has collected data of a different kind from that which is normally published as an International Standard, for example "state of the art".

IEC 62518, which is a technical report, has been prepared by IEC technical committee 68: Magnetic alloys and steels.

The text of this technical report is based on the following documents:

Enquiry draft	Report on voting
68/376/DTR	68/383/RVC

Full information on the voting for the approval of this technical report can be found in the report on voting indicated in the above table.

This publication has been drafted in accordance with the ISO/IEC Directives, Part 2.

The committee has decided that the contents of this publication will remain unchanged until the maintenance result date indicated on the IEC web site under "<http://webstore.iec.ch>" in the data related to the specific publication. At this date, the publication will be

- reconfirmed,
- withdrawn,
- replaced by a revised edition, or
- amended.

A bilingual version of this publication may be issued at a later date.

INTRODUCTION

SmCo_5 was the first sintered rare earth magnet to be developed (1967) [1]¹, followed by $\text{Sm}_2\text{Co}_{17}$ [2, 3, 4] and Nd-Fe-B [5]. These magnets are used in a wide variety of applications. Recently, these magnets have been used in higher temperature applications such as in heavy duty permanent magnet motors. For these high temperature applications, the temperature stability of the permanent magnet has to be considered along with the design of the magnetic circuit. This is particularly relevant for the relatively inexpensive Nd-Fe-B magnetic material which has a comparatively low Curie temperature. The temperature stability of the rare earth sintered magnets has a critical influence on the reliability of high temperature motors and this will, in turn, contribute to energy savings in the future.

Therefore, the subject of this technical report will be of considerable interest to the manufacturers of this type of motor and to the developers of permanent magnet materials.

¹ The figures in square brackets refer to the Bibliography.

RARE EARTH SINTERED MAGNETS – STABILITY OF THE MAGNETIC PROPERTIES AT ELEVATED TEMPERATURES

1 Scope

The scope of this technical report is to describe the temperature behaviour of rare earth sintered magnets in detail for use in designing magnetic circuits exposed to elevated temperatures. The temperature behaviour of SmCo_5 , $\text{Sm}_2\text{Co}_{17}$ and Nd-Fe-B sintered magnets is described.

The various changes of open circuit flux which can occur due to temperature are discussed in Clause 4. The long term stability of the magnets is discussed in Clause 5. The experimental procedures are described in Clause 6. Results of the measurements of the flux loss occurring at the ambient temperature after heating isothermally at 50 °C, 75 °C, 100 °C, 125 °C, 150 °C and 200 °C for up to 1000 h are given in Clause 7. The effect of length to diameter ratio (L/D) of the magnet samples and the influence of H_{cJ} on the flux loss were also studied. The results are discussed in Clause 8.

The data in this technical report was provided by the Institute of Electrical Engineers of Japan (IEEJ) and its subcommittees. This data has been gathered from the members of these subcommittees.

The temperature stability correlated with the complex corrosion behaviour and the spin re-orientation phenomena at cryogenic temperatures will not be given in this technical report.

2 Normative references

IEC 60050-121, *International Electrotechnical Vocabulary – Part 121: Electromagnetism*

IEC 60050-151, *International Electrotechnical Vocabulary – Part 151: Electrical and magnetic devices*

IEC 60050-221:1990, *International Electrotechnical Vocabulary – Chapter 221: Magnetic materials and components*
Amendment 1 (1993)

IEC 60404-8-1, *Magnetic materials – Part 8-1: Specifications for individual materials – Magnetically hard materials*

3 Terms and definitions

For the purpose of this document, the following terms and definitions apply. In addition, most of the technical terms used in this document are defined in IEC 60050-121, IEC 60050-151, and IEC 60404-8-1 (the product standard).

3.1

magnetic flux loss

the reduction due to an external influence, primarily temperature, in the flux of permanent magnets in a magnetized state, unit of Wb. Three kinds of flux loss, reversible flux loss, irreversible flux loss and permanent flux loss, are used to discuss the temperature stability of rare earth sintered magnets.

3.2

reversible flux loss

a magnetization change which is recovered by the removal of a disturbing influence such as temperature. Irreversible flux loss is the partial demagnetization change caused by the temperature changes. The irreversible flux loss is fully recovered by remagnetization. Permanent flux loss is caused by permanent change in the metallurgical state and is generally time and temperature dependent. The permanent loss cannot be recovered to the initial magnetization value by remagnetization.

3.3

uniformity field strength

H_k

the uniformity field strength (of a magnetically hard material) as defined in IEC 60050-221-02-62 (Amendment 1 (1993)) was originally called “knee field” [6]. H_k is the negative value of the magnetic field strength when the magnetic polarization of a magnetically hard material is brought from saturation to 90 % of the value of the remanent magnetic polarization by a monotonically changing magnetic field.

3.4

reversible temperature coefficient

the reversible temperature coefficient of magnetic flux is the percentage changes in flux per degrees Celsius by the change in temperature, which is reversible. The temperature coefficient is expressed as %/°C. The temperature range must be stated to make them quantify. The reversible temperature coefficient of magnetic flux (denoted as $\alpha(\phi)$) is the quotient of the percentage change of magnetic flux by that change in temperature:

$$\alpha(\phi) = (\phi_\theta - \phi_{\text{ref}}) / \phi_{\text{ref}} \cdot 1 / (\theta - \theta_{\text{ref}})$$

where ϕ_θ and ϕ_{ref} are the flux at temperature θ and θ_{ref} respectively.

Generally rare earth sintered magnets exhibit a non-linear change of flux with temperature.

“Temperature coefficient of B_r (denoted as $\alpha(B_r)$)” can be defined from the temperature dependence of B_r in the temperature range to have the quantitative values. The temperature coefficient of B_r is the quotient of the relative change of B_r due to a change in temperature by that change in temperature:

$$\alpha(B_r) = (B_{r\theta} - B_{r\text{ref}}) / B_{r\text{ref}} \cdot 1 / (\theta - \theta_{\text{ref}})$$

where $B_{r\theta}$ and $B_{r\text{ref}}$ are the B_r at temperature of θ and θ_{ref} respectively. “Temperature coefficient of H_{cJ} (denoted as $\alpha(H_{cJ})$)” can be also defined as mentioned above.

The revised evaluation method for temperature coefficients of B_r and H_{cJ} are given in IEC/TR 61807(1999) in which the temperature dependence of B_r and H_{cJ} is expressed by a quadratic function of temperature, see Annex B. To define the “temperature coefficient” the temperature range must be stated because of the non-linearity of the temperature dependence.

3.5

anisotropy field

H_A

the anisotropy field (denoted as H_A) is the field required to rotate into the hard direction or the field to saturate the material in the hard direction, and it is a measure of the anisotropy. The relationship between H_A , K_u (crystalline anisotropy constant) and M_s (saturation magnetization) is as follows:

$$H_A = 2K_u / \mu_0 M_s$$

4 Classification of magnetic flux loss due to temperature

4.1 Reversible flux loss

The reversible change in the magnetic properties of rare earth magnets as a function of temperature originates from the change in saturation magnetization. Reversible flux loss is a magnetization change which is recovered by the removal of a disturbing influence such as temperature.

4.2 Irreversible flux loss

With irreversible flux loss, after the removal of the disturbing influence, the magnetization does not return to its original value. Examples of the disturbing influence are temperature changes, local temperature fluctuations and magnetic fields. The irreversible flux loss is fully recovered by remagnetization.

4.3 Permanent flux loss

Permanent flux loss is caused by a permanent change in the metallurgical state and is generally time and temperature dependent. Examples are precipitation and growth, oxidation, the annealing effects and radiation damage. The permanent flux loss cannot be recovered to the initial magnetization value by remagnetization.

The various flux losses mentioned above are shown in Figure 1. The figures were schematically presented by R. Tenzer [7, 8]. In Figure 1 the magnetic flux density B vs temperature and demagnetization curves at various temperatures with a certain load line are given to explain the three kinds of losses.

The curves in Figure 1(a) apply only for short temperature excursions, for example from 25°C to θ °C. Magnetic flux density B changes reversibly along a demagnetization curve at various temperatures. $B_d(25) - B_d(\theta)$ is called the “reversible flux loss”. This flux loss is fully recovered by returning the magnet to room temperature.

Curves in Figure 1(b) apply for larger temperature excursions. In this case a part of the flux change will be recovered on cooling, $B_d'(25) - B_d'(\theta)$. The other part, $B_d(25) - B_d'(25)$, can be recovered by remagnetization and is called the “irreversible flux loss”.

When the exposure temperature exceeds several hundred degrees Celsius, changes in the microstructure of the magnet, surface oxidation etc., cause an additional flux loss which will no longer be recovered by remagnetization. $B_d(25) - B_d''(25)$ in Figure 1(c) is called the “permanent flux loss”. The reversible B_d vs θ closely reflects the temperature variation of saturation magnetization and remanence. It is commonly approximated by a straight line and is called “the reversible temperature coefficient”, see 3.4.

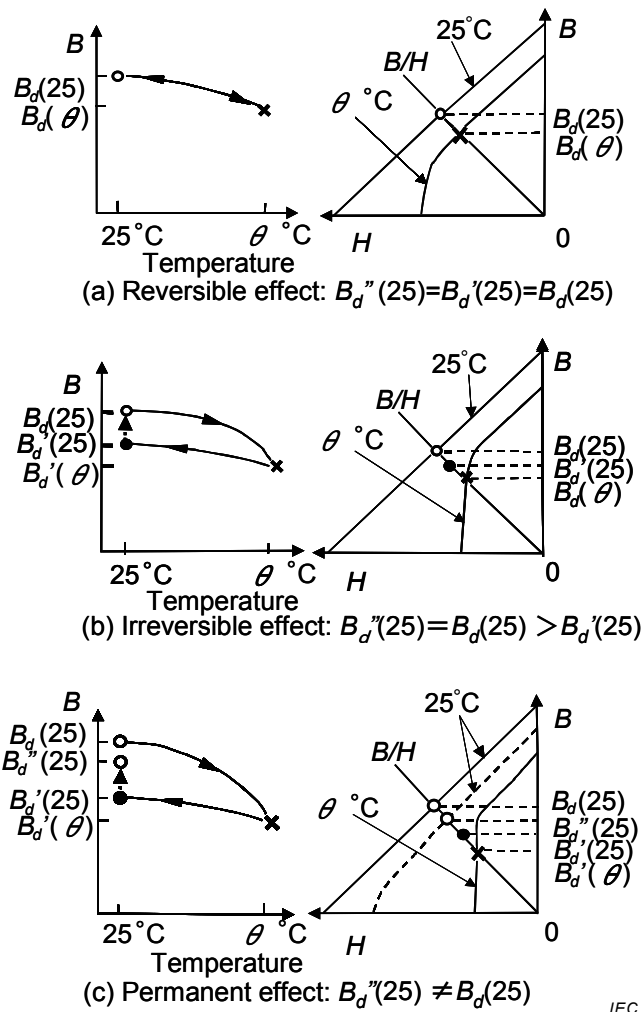


Figure 1 – Change of magnetic flux density operating on a load line during elevated temperature ageing after R. Tenzer (schematic) [7, 8]

5 Long term ageing of rare earth magnets

When a magnet is newly magnetized and the flux (open circuit flux or its operating-point induction) is observed for a long period of time, a slow decay is found to occur. It usually follows a time function. This behaviour is shown in Figure 2 schematically after K. J. Strnat [9].

The change can be separated into three stages. First, there is a relatively fast initial flux loss, ab. This is followed by a long period of increasing stability, marked the “plateau”, bc, during which there is often a constant irreversible flux loss per logarithmic time cycle on the plateau. This time dependency of B on the plateau is proportional to $\log t$ (t is time) from the result of the magnetic after-effect which was given by Street et al. [10]. To show this constant flux change, the “irreversible flux loss per decade” [the flux change per decade (%/decade)] is used. The irreversible flux loss per decade is the flux loss during the time period ranging from 1 h to 10 h, from 10 h to 100 h or from 100 h to 1 000 h.

At higher temperatures and for some magnets, the flux decline, cd, will later accelerate and is sometimes catastrophic. This was observed very clearly for rare earth bonded magnets with an improper surface treatment under harsh environment conditions. For rare earth sintered magnets only small flux changes were observed. The temperature stability correlated with the complex corrosion behaviour will not be given in this technical report.

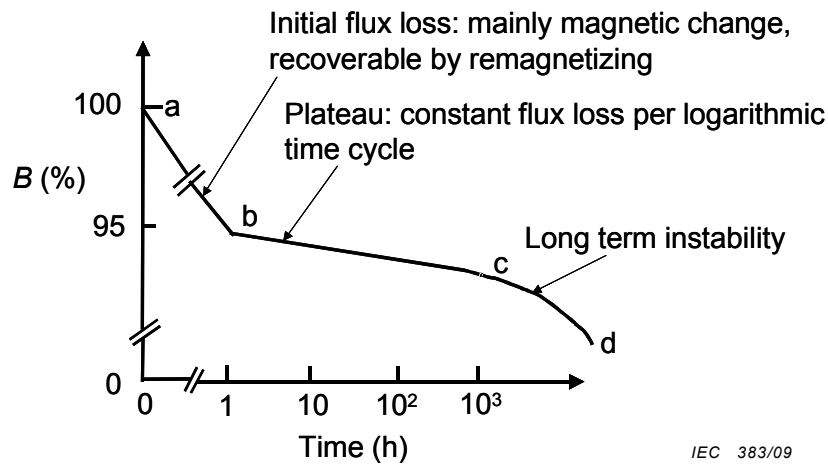


Figure 2 – Long term ageing of rare earth magnets (schematic) [9]

6 Experimental

The dimensions of the specimens used are 10 mm in diameter and 12 mm in length (diameter: D , L : length), $D = 10$ mm and $L = 7$ mm, $D = 10$ mm and $L = 3$ mm and $D = 10$ mm and $L = 2$ mm. The relationship between length to diameter ratio (L/D) and the permeance coefficient (P_c) for cylinders was obtained by Du-Xing Chen et al. [11]. The permeance coefficient is a ratio of the magnetic flux density, B_d , to its self-demagnetisation field, H_d , $P_c = B_d/\mu_0 H_d$.

The initial magnetization was performed with a pulsed magnetic field of 4,1 MA/m to 4,5 MA/m (5,1 T to 5,6 T). The rise time to the peak field was longer than 1 ms. The flux (open circuit flux) was measured with a close fitting pickup coil and a digital integrating fluxmeter. Usually, specimens were pulled out of the close fitting pickup coil. In this experiment, the coil was fixed and specimens passed through the coil [12].

After measuring the flux in the initial state, specimens were kept in an oven with an air atmosphere in which the temperature was controlled to ± 1 °C. Specimens were placed in the oven at a distance of 150 mm from each other to avoid magnetic interaction. During the long term stability tests, the specimens were cooled to room temperature and kept for 1 h before the flux measurement was made. When the temperature changed from 23 °C during the long term flux measurement, the measured flux was corrected using the reversible temperature coefficient.

Irreversible flux losses were evaluated with the following equation:

$$\Delta\phi_{irr} = \{(\phi - \phi_0)/\phi_0\} \times 100 (\%)$$

where

$\Delta\phi_{irr}$ is the irreversible flux loss,

ϕ_0 is the flux in the initial state, and

ϕ is the flux after exposure to the elevated temperature.

Permanent flux losses were determined with the following equation:

$$\Delta\phi_{per} = \{(\phi_{remag} - \phi_0)/\phi_0\} \times 100 (\%)$$

where

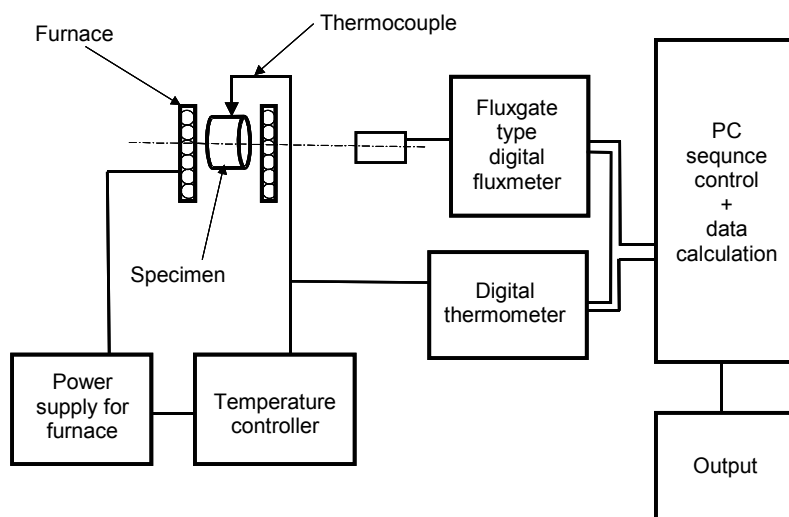
$\Delta\phi_{\text{per}}$ is the permanent flux loss due to structural changes, and

ϕ_{remag} is the flux after remagnetization with a pulsed field of 4,1 MA/m(5,1T).

The temperature coefficient of flux was evaluated by the measurement of temperature dependence of the flux for the magnets in a furnace with a fluxgate type digital integrating fluxmeter. A schematic diagram of the measuring system is shown in Figure 3 [13]. To keep the accuracy in this method, the ambient noise level of the laboratory was evaluated in advance. In this experiment the noise level was less than ± 80 mA/m and the signal was greater than 100 A/m. For the measurement of the flux, specimens of 10 mm in diameter and 7 mm in length were employed. The specimen was set in the furnace at room temperature (23 °C) and heated up to 30 °C. The temperature cycling procedure was heating up to 50 °C from 30 °C at the heating rate of 3 °C/min followed by cooling to 30 °C at the cooling rate of 3 °C/min and heating up to 100 °C followed by cooling to 30 °C and so on (23 °C → 30 °C → 50 °C → 30 °C → 100 °C → 30 °C → 150 °C → 30 °C).

The temperature coefficient of flux determined above is reversible. The temperature dependence of flux on the cooling cycle from 100 °C to 30 °C to determine the reversible temperature coefficient in the temperature range from 30 °C to 100 °C shows the same dependence on heating cycle from 30 °C to 100 °C.

The magnetic properties, B_r , H_{cB} , H_{cJ} and $(BH)_{\text{max}}$, at room temperature were measured with a recording fluxmeter after magnetization in a maximum pulse field of 4,8 MA/m (6,0T). The temperature dependence of the magnetic properties was measured with a vibrating sample magnetometer (VSM) or a recording fluxmeter with an attachment which could control the temperature of a specimen [14]. To measure coercivities of higher than 2 MA/m, a pulse field magnetometer was used [15].



IEC 384/09

Figure 3 – Measuring system of open circuit flux utilizing a fluxgate type digital integrating fluxmeter [13]

7 Temperature stability

7.1 Flux change due to temperature

The changes of flux during temperature cycling for SmCo_5 [16], $\text{Sm}_2\text{Co}_{17}$ [16] and Nd-Fe-B [17] magnets are shown in Figures 4, 5 and 6, respectively. The magnetic properties of the magnets employed for this experiment are summarized in Table 1. The maximum exposure temperatures for SmCo_5 , $\text{Sm}_2\text{Co}_{17}$ and Nd-Fe-B magnets were 200 °C, 200 °C and 150 °C, respectively. Flux changes after exposure at an elevated temperature depend on the temperature, coercivity and the shape of the specimen, L/D for the cylinders. The flux changes of SmCo_5 , $\text{Sm}_2\text{Co}_{17}$ and Nd-Fe-B magnets after exposure to 150 °C are –1,5 %, –3,5 % and –21,1 %, respectively.

Reversible temperature coefficients of magnetic flux can be determined from this data. Reversible temperature coefficients are summarized in Table 2 in which 2 temperature ranges were selected for comparison. The reversible temperature coefficient has a tendency to follow the temperature dependence of saturation magnetization of the magnets. Reversible temperature coefficients of magnetic flux for SmCo_5 , $\text{Sm}_2\text{Co}_{17}$ and Nd-Fe-B magnets are –0,05 %/°C, –0,04 %/°C and –0,13 %/°C, respectively in the temperature range from 30 °C to 100 °C.

Table 1 – Magnetic properties of the rare earth magnets employed for the open circuit flux measurements to determine the reversible temperature coefficient of the magnetic flux

Materials	B_r T	H_{cB} kA/m	H_{cJ} MA/m	$(BH)_{\max}$ kJ/m ³
SmCo_5	0,888	694	1,62	154
$\text{Sm}_2\text{Co}_{17}$	0,96	605	0,721	181
Nd-Fe-B	1,171	897	1,38	260

Table 2 – Reversible temperature coefficient of the magnetic flux determined by temperature cycling

Materials	Reversible temperature coefficient of magnetic flux %/°C (temperature range)	
SmCo_5	–0,0527 ~ –0,0538 (30 °C ~ 100 °C)	–0,0618 (30 °C ~ 200 °C)
$\text{Sm}_2\text{Co}_{17}$	–0,0370 ~ 0,0391 (30 °C ~ 100 °C)	–0,0463 (30 °C ~ 200 °C)
Nd-Fe-B	–0,125 (30 °C ~ 100 °C)	–0,142 (30 °C ~ 150 °C)

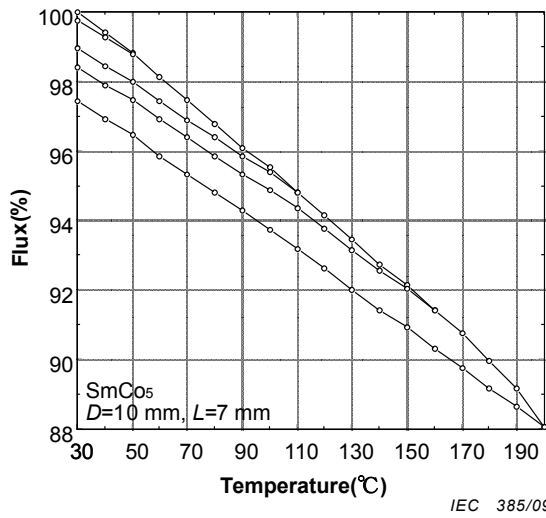


Figure 4 – Temperature dependence of flux for SmCo₅ magnet ($L/D = 0,7$) [16] (See Table 1)

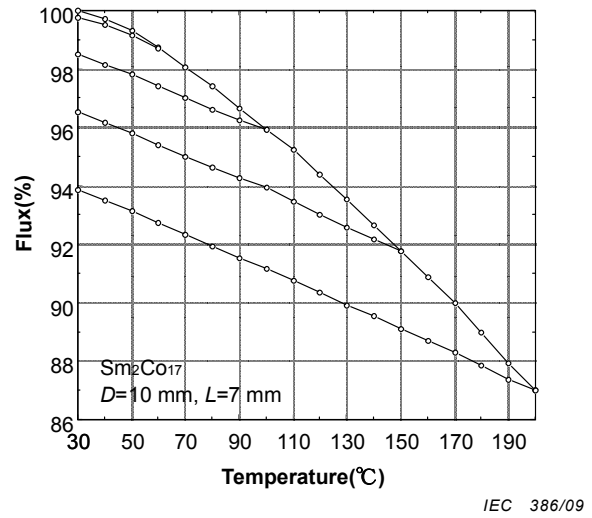


Figure 5 – Temperature dependence of flux for Sm₂Co₁₇ magnet ($L/D = 0,7$) [16] (See Table 1)

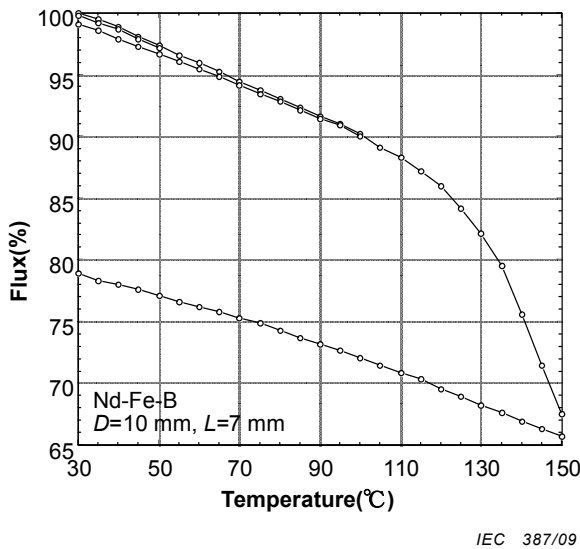


Figure 6 – Temperature dependence of flux for Nd-Fe-B magnet ($L/D = 0,7$) [17] (See Table 1)

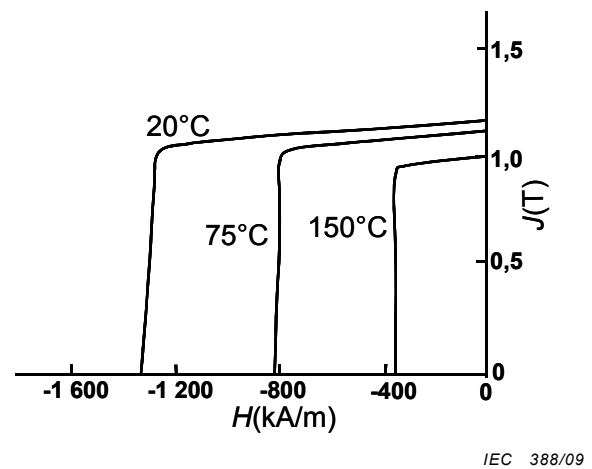


Figure 7 – J - H demagnetization curves of Nd-Fe-B magnet measured at different temperatures [18]

7.2 Effect of temperature on B_r and H_{cJ} (demagnetization curves at different temperatures)

The J - H demagnetization curves of a Nd-Fe-B magnet [18] measured at different temperatures are shown in Figure 7. The temperature dependence of flux for this Nd-Fe-B magnet is also shown in Figure 6. The temperature coefficient of B_r ($\alpha(B_r)$) of a Nd-Fe-B magnet calculated from the data of B_r at 20 °C and 150 °C shown in Figure 6 is $-0,122 \text{ } \%/^{\circ}\text{C}$, which is in sufficient agreement with the reversible temperature coefficient value, $-0,142 \text{ } \%/^{\circ}\text{C}$, as shown in Table 2.

The J - H demagnetization curves at different temperatures of a Nd-Fe-B magnet [18] are shown in Figure 8. The magnetic properties at 25 °C are shown in Table 3. With the data in Figure 8 the temperature dependence of normalized B_r and H_{cJ} for the Nd-Fe-B magnet [19] can be obtained. The same procedure for SmCo_5 and $\text{Sm}_2\text{Co}_{17}$ magnets was followed.

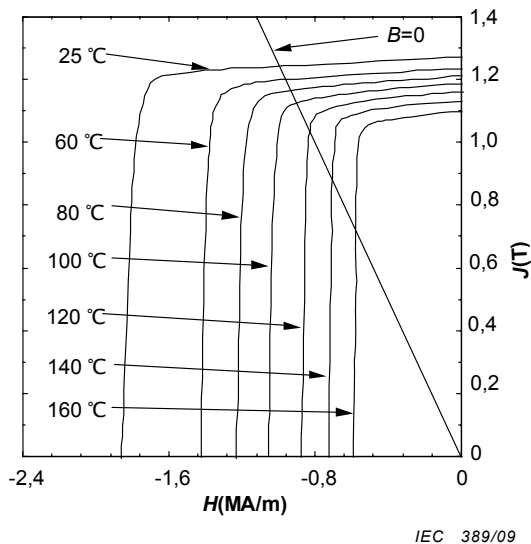


Figure 8 – J - H demagnetization curves of Nd-Fe-B magnet measured at different temperatures [19]

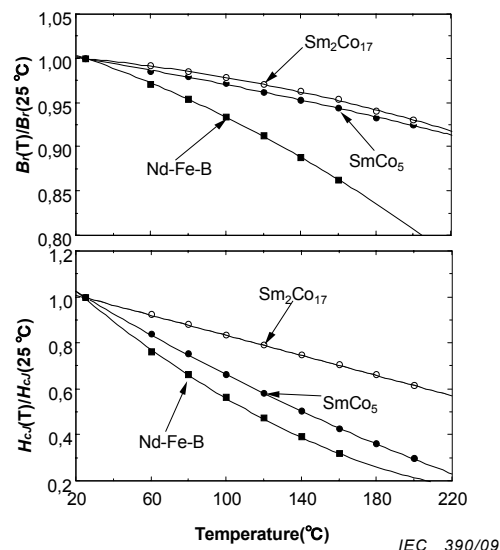


Figure 9 – Temperature dependence of normalized B_r and H_{cJ} for SmCo_5 , $\text{Sm}_2\text{Co}_{17}$ and Nd-Fe-B magnets [19]

Figure 9 shows the temperature dependence of normalized B_r and H_{cJ} for SmCo_5 , $\text{Sm}_2\text{Co}_{17}$ and Nd-Fe-B magnets for which the magnetic properties at 25 °C are shown in Table 3. Values of B_r and H_{cJ} were normalized from the values at 25 °C. The temperature coefficients of B_r and H_{cJ} ($\alpha(B_r)$ and $\alpha(H_{cJ})$) were calculated and are tabulated in Table 3. The value of $\alpha(B_r)$ for the $\text{Sm}_2\text{Co}_{17}$ magnet is the lowest of the three materials. This seems to be explained by the Curie temperature of $\text{Sm}_2\text{Co}_{17}$ magnets being the highest of the three materials.

The non-linearity of the temperature dependence of B_r and H_{cJ} is given in Annex B.

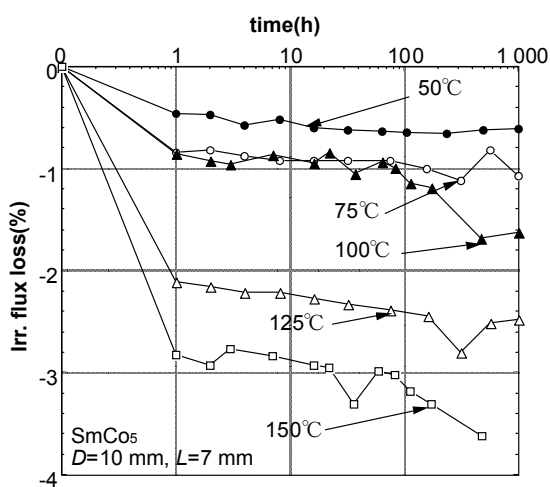
The $\alpha(H_{cJ})$ of the three materials range from $-0,22 \text{ }^\circ\text{C}^{-1}$ to $-0,50 \text{ }^\circ\text{C}^{-1}$, and $-0,22 \text{ }^\circ\text{C}^{-1}$ for $\text{Sm}_2\text{Co}_{17}$ is the lowest. The coercivity of $\text{Sm}_2\text{Co}_{17}$ magnets is controlled by “pinning by precipitates”. The $\alpha(H_{cJ})$ value of $\text{Sm}_2\text{Co}_{17}$ magnets can be controlled by its composition and heat treatment. On the contrary, the $\alpha(H_{cJ})$ of SmCo_5 and Nd-Fe-B magnets cannot be changed significantly because of their coercivity mechanism of “nucleation”. The coercivity of “nucleation” type magnets is determined by the nucleation of a reverse domain after removal of the domain walls, while the movement of existing domain walls within a grain is relatively easy [20, 21].

Table 3 – Temperature coefficients of B_r and H_{cJ} for SmCo_5 , $\text{Sm}_2\text{Co}_{17}$ and Nd-Fe-B magnets (temperature range for the coefficient: 25 °C to 150 °C)

Materials	$\alpha(B_r)$ %/°C	$\alpha(H_{cJ})$ %/°C	Magnetic properties at 25 °C		
			B_r T	H_{cJ} MA/m	$(BH)_{\max}$ kJ/m ³
SmCo_5	–0,042	–0,42	0,964	1,50	179
$\text{Sm}_2\text{Co}_{17}$	–0,034	–0,22	1,085	1,62	222
Nd-Fe-B	–0,10	–0,50	1,280	1,86	316

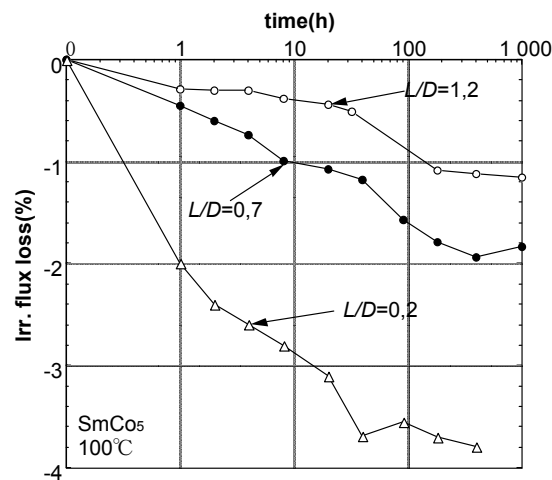
7.3 The time effects at constant temperature (influence of temperature exposure and L/D)

The time dependence of the irreversible flux loss for SmCo_5 [22], $\text{Sm}_2\text{Co}_{17}$ [22] and Nd-Fe-B [23] magnets for various temperatures is shown in Figures 10, 12 and 14, respectively. The magnetic properties of the specimens are shown in Table 4. The initial flux loss generally depends on the coercivity, L/D (length to diameter ratio of cylinders) of the magnet and the exposure temperature. The initial flux losses for SmCo_5 magnets range from –0,46 % to –2,83 % after exposure from 50 °C to 150 °C. The initial flux losses for $\text{Sm}_2\text{Co}_{17}$ magnets range from –0,16 % to –1,86 % after exposure from 50 °C to 150 °C. The initial flux losses for Nd-Fe-B magnets range from –0,16 % to –7,32 % after exposure from 50 °C to 150 °C. There is also a tendency for specimens with a higher initial flux loss to exhibit the higher irreversible flux loss per decade regardless of material.



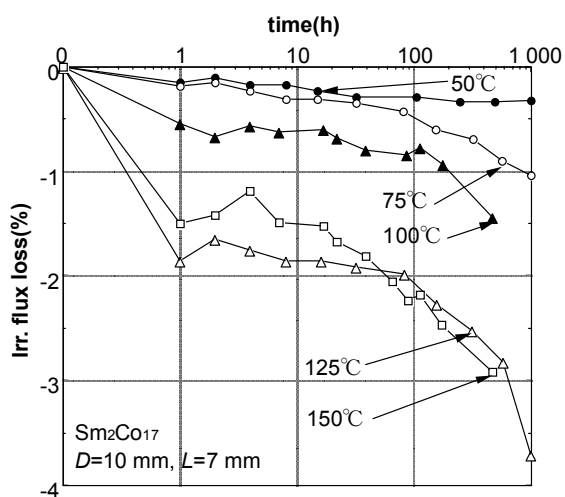
IEC 391/09

Figure 10 – Time dependence of irreversible flux loss for SmCo_5 magnet exposed at different temperatures [22]



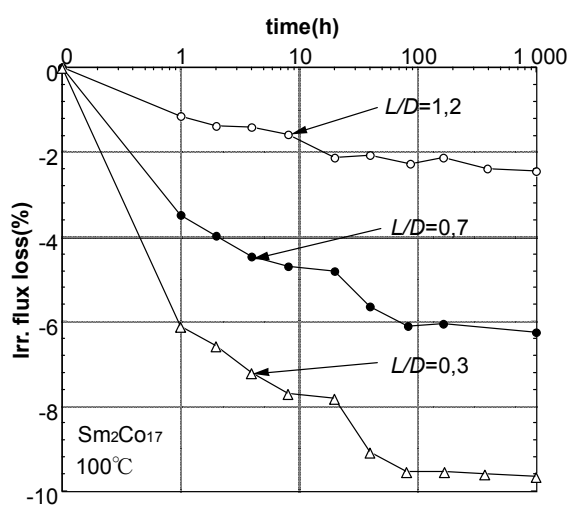
IEC 392/09

Figure 11 – Time dependence of irreversible flux loss for SmCo_5 magnets with various L/D s [24]



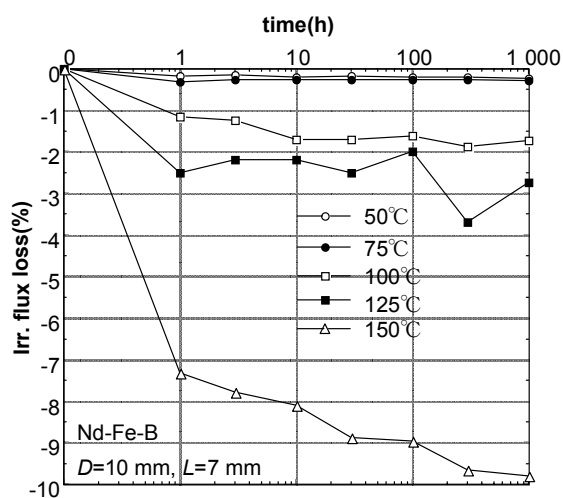
IEC 393/09

Figure 12 – Time dependence of irreversible flux loss for $\text{Sm}_2\text{Co}_{17}$ magnet exposed at different temperatures (Material 1) [22]



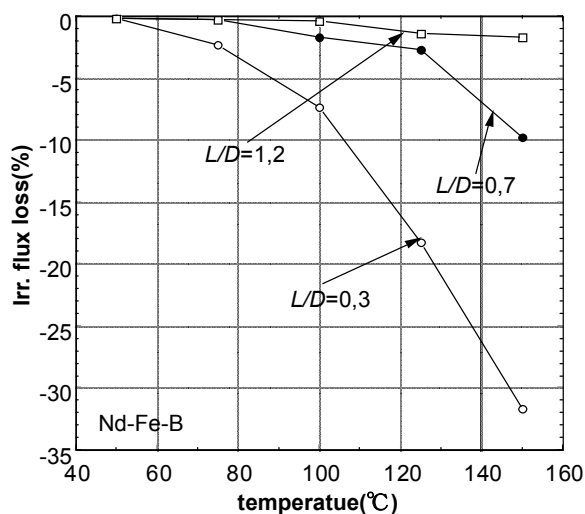
IEC 394/09

Figure 13 – Time dependence of irreversible flux loss for $\text{Sm}_2\text{Co}_{17}$ magnets with various L/D s (Material 2) [24]



IEC 395/09

Figure 14 – Time dependence of irreversible flux loss for Nd-Fe-B magnet exposed at different temperatures [23]



IEC 396/09

Figure 15 – Temperature dependence of irreversible flux loss after exposure for 100 h for Nd-Fe-B magnets with various L/D s [25]

The time dependence of irreversible flux loss for SmCo_5 [24] and $\text{Sm}_2\text{Co}_{17}$ [24] magnets with different L/D values is shown in Figures 11 and 13, respectively. The temperature dependence of irreversible flux loss after exposure for 100 h for Nd-Fe-B [25] magnets with different L/D values is shown in Figure 15. As shown in the data, specimens with the lowest L/D exhibit the highest irreversible flux loss. The lower L/D means that a higher demagnetisation field is applied to magnets by their own magnetization and a higher irreversible flux loss results.

The irreversible flux loss behaviour of rare earth magnets is dependent on H_{cJ} , L/D , exposure temperature and H_k , the uniformity field strength (see 3.3), which is a measure for the squareness of the demagnetization curve. The squareness of the demagnetisation curve is not considered as a parameter to control the irreversible flux loss in this technical report.

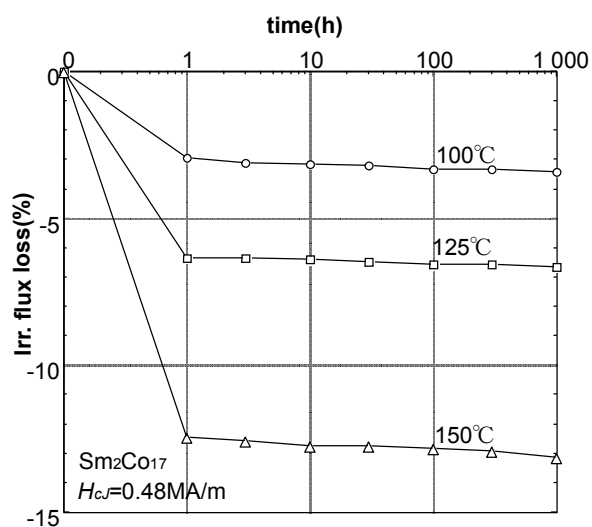
Table 4 – Magnetic properties of the specimens for the experiments to evaluate the effects of temperature and L/D on irreversible flux loss

Materials	B_r T	H_{cB} kA/m	H_{cJ} MA/m	$(BH)_{max}$ kJ/m ³
SmCo ₅	0,90	680~690	0,92~1,15	156~159
Sm ₂ Co ₁₇ -1 (influence of temperature)	0,97	530	0,57	187
Sm ₂ Co ₁₇ -2 (influence of L/D)	1,09	540	0,60	209
Nd-Fe-B	1,171	897	1,38	260

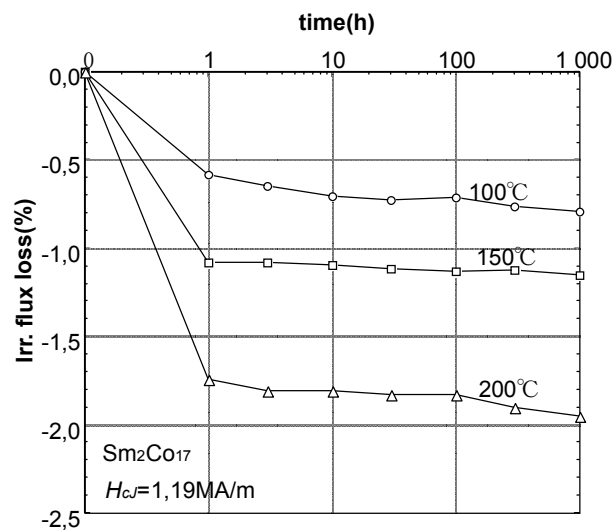
7.4 The influence of H_{cJ} on the irreversible flux loss for Sm₂Co₁₇ magnets

The time dependence of irreversible flux loss for Sm₂Co₁₇ magnets with $H_{cJ} = 0,48$ MA/m [26], 1,19 MA/m [27] and 1,97 MA/m [28] is shown in Figures 16, 17 and 18, respectively. Each plot of irreversible flux loss in the figure is the average of two samples. Using the methods described in references [2], [3] and [4], H_{cJ} can be increased by changes in composition and heat treatment pattern. The magnetic properties of Sm₂Co₁₇ magnets used in the experiment to evaluate the influence of H_{cJ} on the irreversible flux loss are shown in Table 5. High coercivity Sm₂Co₁₇ magnets are relatively difficult to magnetize because of the coercivity mechanism of “pinning”. The coercivity of “pinning” type magnets is determined by the pinning of the domain walls at the phase boundary of the precipitate and the further movement of domain walls is strongly impeded by pinning, while small reverse domains exist at all times [20, 29]. From the data in Figures 16, 17 and 18, it is concluded that irreversible flux loss can be reduced by an increase in coercivity under conditions which retain the squareness level.

Comparison of the irreversible flux losses for Sm₂Co₁₇ magnets with different H_{cJ} is shown in Figure 23. The irreversible flux losses shown in Figure 23 are after an exposure for 1 000 h. Increasing the H_{cJ} from 0,48 MA/m to 1,97 MA/m reduces the irreversible flux loss from –13 % to –1 % on exposure to 200 °C for 1 000 h. The coercivity enhancement of Sm₂Co₁₇ magnets improves the temperature stability remarkably and the Sm₂Co₁₇ magnets show the best temperature stability among the three materials.



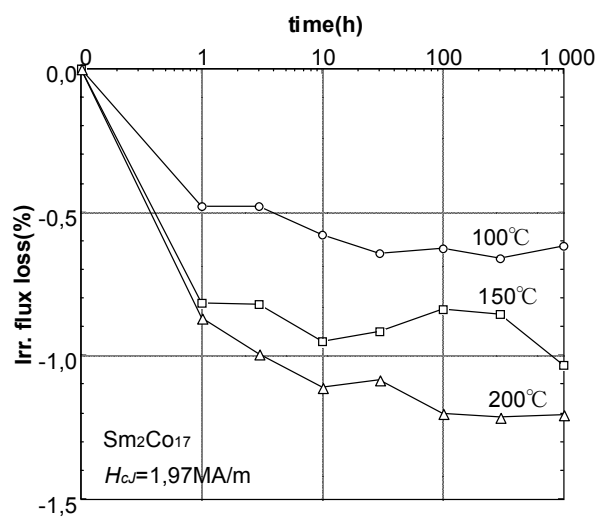
IEC 397/09



IEC 398/09

Figure 16 – Time dependence of irreversible flux loss for a $\text{Sm}_2\text{Co}_{17}$ magnet with $H_{cJ} = 0,48 \text{ MA/m}$ and $L/D = 0,7$ [26]

Figure 17 – Time dependence of irreversible flux loss for a $\text{Sm}_2\text{Co}_{17}$ magnet with $H_{cJ} = 1,19 \text{ MA/m}$ and $L/D = 0,7$ [27]



IEC 399/09

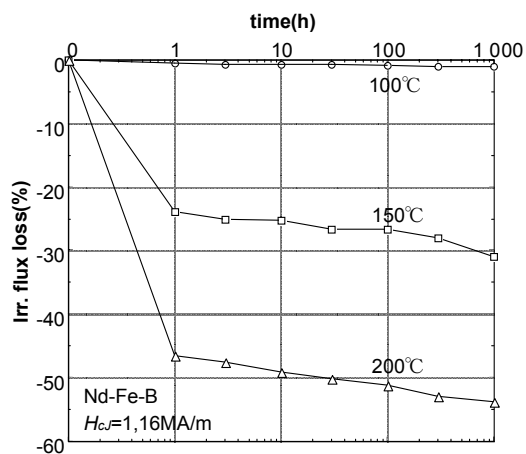
Figure 18 – Time dependence of irreversible flux loss for a $\text{Sm}_2\text{Co}_{17}$ magnet with $H_{cJ} = 1,97 \text{ MA/m}$ and $L/D = 0,7$ [28]

Table 5 – Magnetic properties of the $\text{Sm}_2\text{Co}_{17}$ magnets for the experiment to evaluate the influence of H_{cJ} on the irreversible flux loss

No.	B_r T	H_{cB} kA/m	H_{cJ} MA/m	$(BH)_{\max}$ kJ/m ³
1	1,05	449	0,48	192
2	1,10	792	1,19	221
3	1,12	818	1,97	232

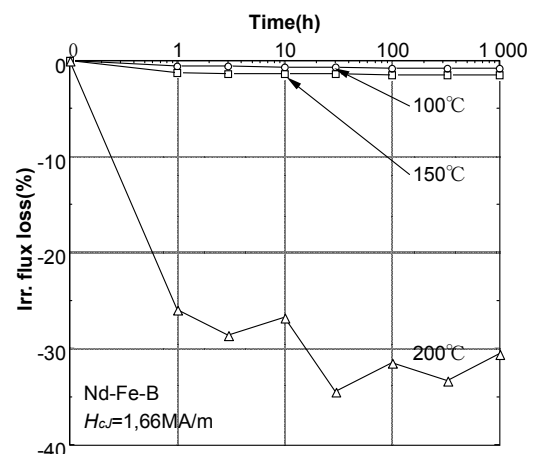
7.5 The influence of H_{cJ} on the irreversible flux loss for Nd-Fe-B magnets

The time dependence of irreversible flux loss for Nd-Fe-B magnets with $H_{cJ} = 1,16$ MA/m [30], 1,66 MA/m [31], 2,17 MA/m [32] and 2,45 MA/m [33] are shown in Figures 19, 20, 21 and 22, respectively. Looking at these figures, we see that the magnets with the higher coercivity exhibit a less irreversible flux loss. The coercivity of Nd-Fe-B magnets may be increased by the substitution of Dy or Tb for Nd; however, there is a subsequent reduction of B_r with this substitution. The magnetic properties of the Nd-Fe-B magnets for the evaluation of the effect of H_{cJ} are shown in Table 6. The H_{cJ} improvement is obtained by the considerable substitute of other rare earths with the sacrifice of B_r .



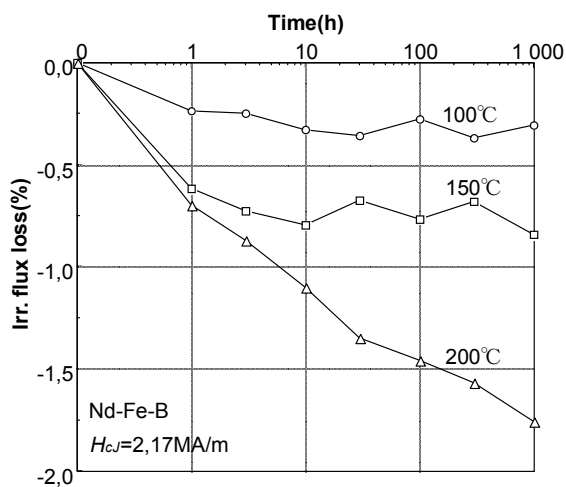
IEC 400/09

Figure 19 – Time dependence of irreversible flux loss for a Nd-Fe-B magnet with $H_{cJ} = 1,16$ MA/m and $L/D = 0,7$ [30]



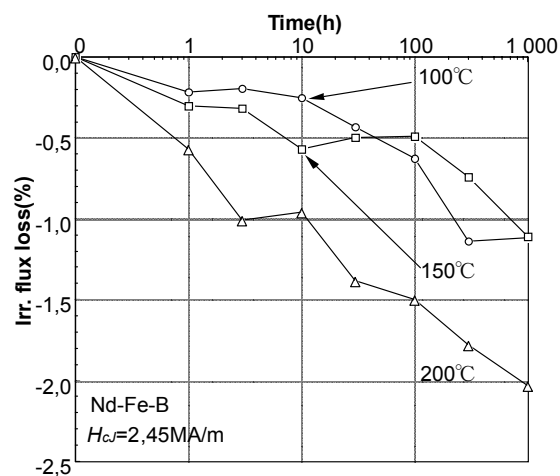
IEC 401/09

Figure 20 – Time dependence of irreversible flux loss for a Nd-Fe-B magnet with $H_{cJ} = 1,66$ MA/m and $L/D = 0,7$ [31]



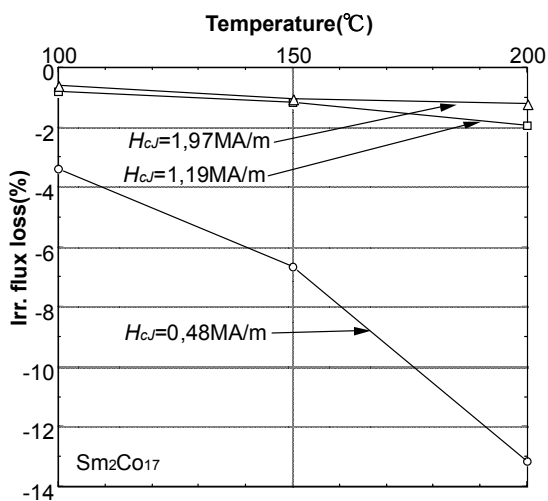
IEC 402/09

Figure 21 – Time dependence of irreversible flux loss for a Nd-Fe-B magnet with $H_{cJ} = 2,17$ MA/m and $L/D = 0,7$ [32]



IEC 403/09

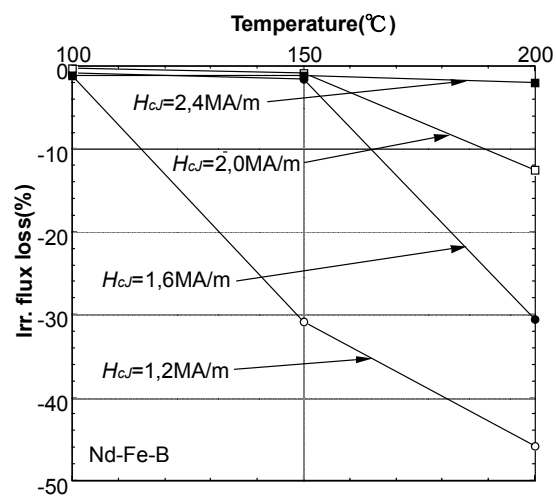
Figure 22 – Time dependence of irreversible flux loss for a Nd-Fe-B magnet with $H_{cJ} = 2,45$ MA/m and $L/D = 0,7$ [33]



IEC 404/09

The irreversible flux losses were measured after holding the sample at a certain temperature for 1 000 h.

Figure 23 – Comparison of irreversible flux loss for $\text{Sm}_2\text{Co}_{17}$ magnets with different H_{cJ}



IEC 405/09

The irreversible flux losses were measured after holding the sample at a certain temperature for 1 000 h.

Figure 24 – Comparison of irreversible flux loss for Nd-Fe-B magnets with different H_{cJ}

A comparison of the irreversible flux losses for Nd-Fe-B magnets with different H_{cJ} values is shown in Figure 24. An increase of H_{cJ} from 1,16 MA/m to 2,45 MA/m improves the irreversible flux loss from -43 % to -2 % after exposure at 200 °C for 1 000 h.

At this time the $\alpha(H_{cJ})$ of Nd-Fe-B magnets has not been improved, though investigations have been made. Magnets with a higher coercivity up to 2,8 MA/m have been developed and used for high temperature applications.

A summary of the temperature stability graphs is given in Table A.1.

Table 6 – The magnetic properties of Nd-Fe-B magnets for the evaluation of the influence of H_{cJ} on irreversible flux loss measured by a pulse recording fluxmeter

No.	B_r T	H_{cB} kA/m	H_{cJ} MA/m	$(BH)_{max}$ kJ/m ³	H_A MA/m
1	1,324	980	1,16	324	7,07
2	1,238	934	1,66	287	7,78
3	1,179	909	2,17	276	9,74
4	1,154	886	2,45	254	9,74

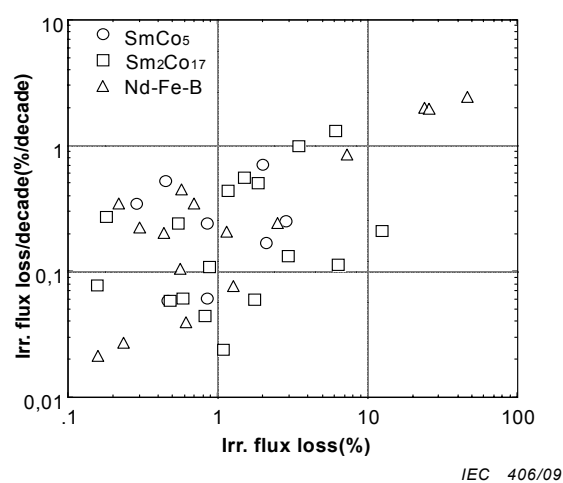
7.6 Irreversible flux loss per decade

The relationship between the irreversible flux loss per decade and the initial flux loss is shown in Figure 25. The data in this figure were collected from the data on the time dependence of irreversible flux loss in this technical report. The values of the “irreversible flux loss per decade” were determined by a least square fit using irreversible flux loss data for 1 h to 1000 h. The irreversible flux loss per decade is dependent on the initial flux loss value, that is, the magnets with the higher initial flux loss exhibit the higher irreversible flux loss per decade. There is no significant difference in the irreversible flux loss per decade between the three materials. The origin of this tendency in the irreversible flux loss per decade of the sintered magnets has not been clearly understood.

7.7 Permanent flux loss

The permanent flux loss of Sm_2Co_{17} and Nd-Fe-B magnets after exposure at 100 °C to 200 °C for 1000 h is tabulated in Tables 7 and 8. The permanent flux loss for Sm_2Co_{17} magnet ranges from –1,15 % to +0,377 % and sometimes an increase in flux was observed. The permanent flux loss seems to be due to a change of the morphology of the precipitate and/or oxidation. The permanent flux loss for Nd-Fe-B magnets after exposure at 100 °C to 200 °C for 1000 h ranges from –1,1 % to +0,14 % and seems to be coming from the oxidation of $R_2Fe_{14}B$ (R: rare earth elements) main phase and the R rich phase. The results are not so systematic but absolute values of the permanent flux loss are distributed around 1 %. It is concluded that magnets exposed at the higher temperatures exhibit the higher permanent loss.

The thickness of surface oxidized layer for (Nd, Dy)-Fe-B sintered magnets is proportional to $t^{1/2}$ (t is the exposure time in seconds) [34]. The results on the permanent flux loss are consistent with a $t^{1/2}$ law on the oxidation behaviour of (Nd, Dy)-Fe-B sintered magnets. The calculated thickness of surface oxidized layer is less than 1 µm after an exposure at 200 °C for 1 000 h.



NOTE All data in this figure are collected from the figures on time dependence of irreversible flux loss in this technical report.

Figure 25 – Relationship between irreversible flux loss per decade and initial flux loss

Table 7 – The permanent flux loss of $\text{Sm}_2\text{Co}_{17}$ magnets after exposure for 1 000 h at different temperatures

H_{cJ} MA/m	Permanent flux loss %					
	Exposed at 100 °C		Exposed at 150 °C		Exposed at 200 °C	
0,48	+0,16	+0,26	+0,04	+0,16	–0,08	+0,012
1,19	–1,08	–1,15	+0,02	+0,03	+0,377	+0,012
1,97	+0,04	+0,16	–0,02	–0,01	–0,27	–0,09

NOTE The specimens were remagnetized after the experiments shown in Figures 16 to 18.

Table 8 – The permanent flux loss of Nd-Fe-B magnets after exposure for 1 000 h at different temperatures

H_{cJ} MA/m	Permanent flux loss %					
	Exposed at 100 °C		Exposed at 150 °C		Exposed at 200 °C	
1,16	–0,54	–0,58	–0,17	+0,14	–0,85	–1,10
1,66	–0,41	–0,34	–0,14	–0,30	++	++
2,17	–0,01	–0,22	–0,28	–0,55	–0,16	----
2,45	–0,21	–0,23	–0,18	–0,68	–0,55	–0,47

++ : Permanent loss increased but exact values were not obtained.

NOTE The specimens were remagnetized after the experiments shown in Figures 19 to 22.

8 Summary

The temperature characteristics of SmCo_5 , $\text{Sm}_2\text{Co}_{17}$ and Nd-Fe-B sintered magnets are closely dependent on the magnetic properties and the temperature dependence of the base intermetallic compounds as shown in Table 9. The temperature stability of $\text{Sm}_2\text{Co}_{17}$ sintered magnets is the best among the three kinds of rare earth sintered magnets taking account of the three parameters T_c , $\alpha(B_r)$ and $\alpha(H_{cJ})$ while sintered Nd-Fe-B material remains, by far, the preferred material for permanent magnet applications.

For Nd-Fe-B sintered magnets, the value of $\alpha(B_r)$ can be improved by Co substitution, but excess substitution decreases the crystalline anisotropy and H_{cJ} . The only way to improve the thermal stability of a Nd-Fe-B sintered magnet is to increase H_{cJ} , because there is no feasible method to decrease $\alpha(H_{cJ})$.

For the best temperature stability of rare earth sintered magnets, a high coercivity and good squareness of the demagnetization curve are required.

The results described in this technical report are for the rare earth sintered magnets exposed to dry air environments. It is noteworthy that the results for the magnets exposed to humid environments will be different from those described in the technical report.

Table 9 – Basic magnetic properties of the three intermetallic compounds

Materials	Crystal structure	Basic magnetic properties of intermetallic compound			
		Saturation magnetization M_s T	Curie temperature T_c °C	Crystalline anisotropy constant K_u MJ/m ³	Anisotropy field H_A MA/m
SmCo_5 [20]	Hexagonal	1,14	727	11~20	20~35
$\text{Sm}_2\text{Co}_{17}$ [20]	Rhombohedral	1,25	920	3,2	5,2
$\text{Nd}_2\text{Fe}_{14}\text{B}$ [35]	Tetragonal	1,60	315	5,0	6,0

Annex A (informative)

Summary of temperature stability graphs

The graphs to elucidate the temperature stability for three kinds of rare earth sintered magnets are summarised in Table A.1.

Table A.1 – Summary of temperature stability graphs

Figure	Magnet materials	Magnet L/D	Time h	Temperature °C
10	SmCo_5	0,7	1 000	50, 75, 100, 125, 150
11	SmCo_5	1,2 0,7 0,2	1 000	100
12	$\text{Sm}_2\text{Co}_{17}$	0,7	1 000	50, 75, 100, 125, 150
13	$\text{Sm}_2\text{Co}_{17}$	1,2 0,7 0,3	1 000	100
14	Nd-Fe-B	0,7	1 000	50, 75, 100, 125, 150
15	Nd-Fe-B	1,2 0,7 0,3	100 Irreversible flux loss vs temperature	Up to 150
16	$\text{Sm}_2\text{Co}_{17}$	0,7	1 000	100, 150, 200
17	$\text{Sm}_2\text{Co}_{17}$	0,7	1 000	100, 150, 200
18	$\text{Sm}_2\text{Co}_{17}$	0,7	1 000	100, 150, 200
19	Nd-Fe-B	0,7	1 000	100, 150, 200
20	Nd-Fe-B	0,7	1 000	100, 150, 200
21	Nd-Fe-B	0,7	1 000	100, 150, 200
22	Nd-Fe-B	0,7	1 000	100, 150, 200
23	$\text{Sm}_2\text{Co}_{17}$	Irreversible flux loss vs temperature (parameter: H_{cJ})		
24	Nd-Fe-B	Irreversible flux loss vs temperature (parameter: H_{cJ})		

Annex B (informative)

Non-linearity of temperature dependence of B_r and H_{cJ}

A concrete illustration to show the non-linearity of the temperature dependence of B_r and H_{cJ} is given in Figure B.1. The temperature dependence is expressed with a quadratic function of temperature. The quadratic functions are

$$B_r(\theta)/B_r(25\text{ °C}) = -2,24 \times 10^{-6} \theta^2 - 6,02 \times 10^{-4} \theta + 1,02 \text{ and}$$

$$H_{cJ}(\theta)/H_{cJ}(25\text{ °C}) = 1,33 \times 10^{-5} \theta^2 + 7,45 \times 10^{-3} \theta + 1,17$$

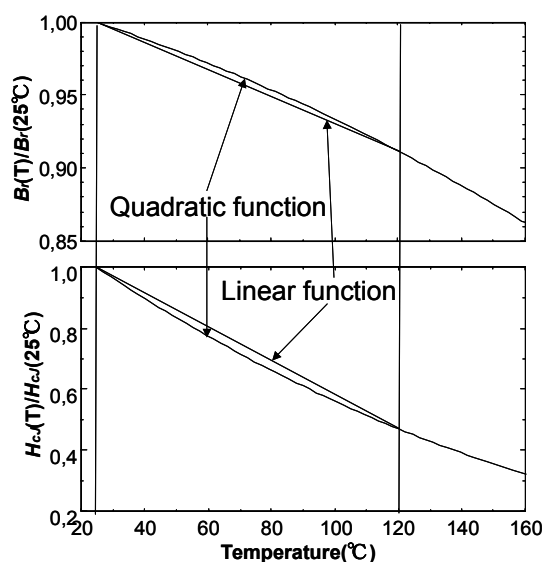
for a temperature dependence of B_r and H_{cJ} , respectively. A straight line drawn between 25 °C and 120 °C shows clearly that the temperature dependence of B_r and H_{cJ} is not linear. In this case, θ and θ_{ref} are 120 °C and 25 °C, respectively.

The linear functions are

$$B_r(\theta)/B_r(25\text{ °C}) = -9,24 \times 10^{-4} \theta + 1,02 \text{ and}$$

$$H_{cJ}(\theta)/H_{cJ}(25\text{ °C}) = -5,52 \times 10^{-3} \theta + 1,14$$

for a temperature dependence of B_r and H_{cJ} , respectively. Calculated temperature coefficients $\alpha(B_r)$ and $\alpha(H_{cJ})$ in the temperature range from 25 °C to 120 °C using the linear functions are $-0,092\text{ %/°C}$ and $-0,55\text{ %/°C}$, respectively.



IEC 407/09

Figure B.1 – Temperature dependence of normalized B_r and H_{cJ} to show the non-linearity (see data for Nd-Fe-B magnets in Figure 9)

Bibliography

- [1] M. G. Benz and D. L. Martin, J. Appl. Phys., 39, 1717 (1968).
- [2] H. Senno and Y. Tawara, Japn. J. Appl. Phys., 14, 1619 (1975).
- [3] T. Ojima, S. Tomizuka, T. Yoneyama and T. Hori, IEEE Trans. Magn., MAG-13, 1317 (1977).
- [4] T. Yoneyama, A. Fukuno and T. Ojima, Proc. ICF3, p. 97 (1980).
- [5] M. Sagawa, S. Fujimura, N. Togawa, H. Yamamoto and Y. Matsuura, J. Appl. Phys., 55, 2083 (1984).
- [6] D. L. Martin and M. G. Benz, IEEE Trans. Magn., vol. MAG-8, 35 (1972).
- [7] R. Tenzer: "Temperature Effects on Permanent Magnets", Applied Magnetism, Vol. 16, No. 1, Company Journal of the Indiana General Div., EM & M Corp., Valparaiso, Indiana (1969).
- [8] R. J. Parker: "Advances in Permanent Magnetism", John Wiley & Sons, p.105 (1990).
- [9] K. J. Strnat, "Study and Review of Permanent Magnets for Electric Vehicle Propulsion Motors", NASA CR-168178 DOE/NASA/0189-83/2, p. 3-24 (September, 1983).
- [10] R. Street and J. Wooley, Proc. Phys. Soc. London A62, 562 (1949).
- [11] Du-Xing Chen and J. A. Brug, IEEE Trans. Magn., vol. 27, 3601 (1991).
- [12] Technical Report of IEEJ, No. 239, p. 4 (1987) (in Japanese).
- [13] Technical Report of IEEJ, No. 239, p. 33 (1987) (in Japanese).
- [14] Technical Report of IEEJ, No. 484, p. 4 (1994) (in Japanese).
- [15] G. Kido, Y. Nakagawa, T. Ariizumi, H. Nishio and T. Takano, Proc. 10th Int'l Workshop on Rare Earth Magnets and their Applications, Kyoto, p.101 (1989).
- [16] Technical Report of IEEJ, No. 239, p. 37 (1987) (in Japanese).
- [17] Technical Report of IEEJ, No. 484, p. 36 (1994) (in Japanese).
- [18] Technical Report of IEEJ, No. 484, p. 5 (1994) (in Japanese).
- [19] Proc. of Technical Symposium on Magnetic Applications, Makuhari, Japan, 2-1 (1999) (in Japanese).
- [20] K. J. Strnat, Ferromagnetic Materials, Vol. 4, Edited by E. P. Wohlfarth and K. H. J. Buschow, p. 131, Elsevier Science Publishers B. V. (1988).
- [21] H. Kronmuller, phys. Stat. Sol. (b), 130, 197 (1985).
- [22] Technical Report of IEEJ, No. 239, p. 14 (1987) (in Japanese).
- [23] Technical Report of IEEJ, No. 484, p. 21 (1994) (in Japanese).
- [24] Technical Report of IEEJ, No. 239, p. 17 (1987) (in Japanese).
- [25] Technical Report of IEEJ, No. 484, p. 24 (1994) (in Japanese).
- [26] Data of IEEJ, No. HP-20, 43 and 45 (2004 and 2005) (in Japanese).
- [27] Data of IEEJ, No. HP-37, 46 and 47 (2004 and 2005) (in Japanese).
- [28] Data of IEEJ, No. HP-40, 48 and 49 (2004 and 2005) (in Japanese).

- [29] K. D. Durst and H. Kronmuller, J. Magn. & Magn. Matr., 68, 63 (1987).
 - [30] Technical Report of IEEJ, No. 1011, p. 11 (2005) (in Japanese).
 - [31] Technical Report of IEEJ, No. 1011, pp. 11 and 12 (2005) (Summarized Figs. 3.4, 3.5 and 3.6) (in Japanese).
 - [32] Technical Report of IEEJ, No. 1011, p. 12 (2005) (Summarized Figs. 3.7, 3.8 and 3.9) (in Japanese).
 - [33] Technical Report of IEEJ, No. 1011, pp. 12 and 13 (2005) (Summarized Figs. 3.10, 3.11 and 3.12) (in Japanese).
 - [34] R. Blank and E. Adler, Proc. of 9th Intl. Workshop on Rare Earth Magnets and Their Applications, Bad Soden, FRG, p. 537 (1987).
 - [35] K. H. J. Buschow, Ferromagnetic Materials, Vol. 4, Edited by E. P. Wohlfarth and K. H. J. Buschow, p. 1, Elsevier Science Publishers B. V. (1988).
 - [36] IEC/TR 61807:1999, *Magnetic properties of magnetically hard materials at elevated temperatures – Methods of measurement*
-

INTERNATIONAL
ELECTROTECHNICAL
COMMISSION

3, rue de Varembé
PO Box 131
CH-1211 Geneva 20
Switzerland

Tel: + 41 22 919 02 11
Fax: + 41 22 919 03 00
info@iec.ch
www.iec.ch